

$$h_{23} + h_{34} = 2h_{34}$$

$$h_{12} + h_{23} + h_{34} = 3h_{34} - 4.5$$

i.e.

$$h_{23} = h_{34}$$

$$h_{12} = h_{34} - 4.5 \quad (2)$$

Equations 1 and 2 are consistent if

$$t_3 = 0.5(t_2 + t_4)$$

$$t_4 - t_2 - t_3 = 4.5 \quad (3)$$

The close agreement between the estimates of t_4 given by the ab initio¹⁵ (14 kcal/mol) and MM2¹⁴ (13 kcal/mol) calculations indicate that the true value must be close to 13.5 kcal/mol. If so, then

$$t_2 = 1.5; t_3 = 7.5 \text{ kcal/mol} \quad (4)$$

The small value for t_2 seems very reasonable because two of the bridges in **2t** favor the untwisted geometry. The corresponding saturated bridge should relax further in **3t**, and the two saturated bridges in **3t** should relax further in **4t**. The values for the twisting energies in eq 4 also agree with our MM2 estimates (4.0, 7.9, and 13.0 kcal/mol, respectively) within the combined error limits of experiment and MM2. Thus the results reported by LPPR⁷ can be interpreted satisfactorily in terms of a model where **1** is *not* stabilized by homoaromaticity, the difference between the heat of hydrogenation of **1** to **2t** and that of **2t** to **3t** or of **3t** to **4t** being due to differences in the twisting energies.

Conclusions

The calculations and arguments presented here strongly imply that triquinacene (**1**) is *not* an aromatic species, the effects of homoconjugation on its energy being very small. This is satis-

factory because it is very difficult to see how homoconjugative interactions could lead to significant stabilization in a neutral cyclic conjugated hydrocarbon with an even numbered ring and three "long" (2.51 Å) CC bonds. LPPR⁷ arrived at an erroneous conclusion in this connection because they failed to consider the effects of twisting in **2-4**. Their results can be explained quantitatively in this way.

Note that this conclusion is not inconsistent with evidence⁶ from UPE spectroscopy, showing that interactions between the π MO's of **2** leads to significant changes in orbital energies. The interactions that lead to these changes correspond¹⁶ to first-order perturbations involving mutual interaction between the three degenerate π MO's. While such first-order interactions can lead to significant changes in the MO energies, they do *not* lead to overall stabilization.¹⁶

While Miller et al.⁸ have also concluded that **1** is not homoaromatic, their ab initio calculations disagree with experiment in predicting the heats of hydrogenation for each of the four steps in the conversion of **1** to **4t** to be the same. Discrepancies of this kind are nearly always due to errors in the calculated values and the work reported above makes it seem almost certain that this is the case here. Errors of this magnitude in heats of formation calculated by the procedures used by Miller et al.⁸ are by no means unknown.

Acknowledgment. This work was supported by the Air Force Office for Scientific Research (Grant AFOSR 86-0022), the Robert A. Welch Foundation (Grant F-126), and the National Science Foundation (Grant CHE 87-12022). The ab initio calculations were carried out using the CRAY X-MP/24 computer at The University of Texas Center for High Performance Computing.

(16) Dewar, M. J. S.; Dougherty, R. C. *The PMO Theory of Organic Chemistry*; Plenum: New York, 1975.

Sesquibicyclic Hydrazines: Oxidation Thermodynamics and Cation Radical Nitrogen ESR Splittings and UV Absorption Maxima

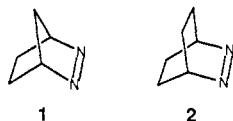
Stephen F. Nelsen,* Timothy B. Frigo, and Yaesil Kim

Contribution from the S. M. McElvain Laboratories of Organic Chemistry, Department of Chemistry, University of Wisconsin, Madison, Wisconsin 53706. Received October 27, 1988. Revised Manuscript Received February 7, 1989

Abstract: Diels-Alder addition of 1,3-cyclohexadiene to protonated 3,4-diazatricyclo[4.2.1.0^{2,5}]non-3-ene (**3**), 2,3-diazabicyclo[2.1.1]hex-2-ene (**4**), and 6,7-diazabicyclo[3.2.2]non-6-ene (**5**) gave **8**, **6**, and **9**, respectively, and addition of 1,3-cycloheptadiene to **5** gave **10**. The saturated compounds **7**, **11**, and **12** were prepared by hydrogenating **6**, **9**, and **10**. Comparisons of E° , vIP, cation radical ESR nitrogen splitting constants [$a(N)$], and UV absorption maxima with values for other sesquibicyclic hydrazines and with AM1 semiempirical calculations are discussed. The double nitrogen inversion barrier of **7^{•+}** was determined by ESR to be 4.6 kcal/mol, within experimental error of that previously measured for **16-d₁₂^{•+}**. Changing bicyclic ring size in sesquibicyclic hydrazines greatly affects the ease of oxidation and cation radical properties. Changes in ΔG° for first electron loss are usefully described as one dimensional in nitrogen pyramidalities caused by the rings present regardless of their identity (using $\alpha(av)$ calculated by AM1). Calculation of nitrogen ESR splitting constants for the cation radicals requires averaging over the energy surface for bending at nitrogen. This problem is less well described as one dimensional in $\alpha(av)$ as the ring sizes are enlarged, and $a(N)$ is calculated to be modestly sensitive to the identity of the bicyclic rings. Cation radical UV absorption spectra are not calculated usefully by semiempirical methods. The identity of the rings and not simply nitrogen pyramidalities is clearly of importance, and this is not handled accurately enough by available calculations.

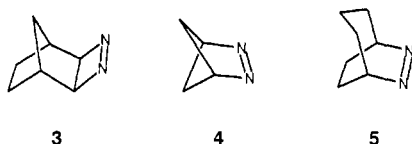
Protonated bicyclic azo compounds **1** and **2** undergo Diels-Alder addition to cyclic 1,3-dienes to give protonated bis-N,N'-

bicyclic ("sesquibicyclic") hydrazines.¹ The neutral adducts are thermally unstable to retro-Diels-Alder cleavage, and no adduct



could be detected in equilibrium with its components, so the additions are endothermic in the absence of acid. The substantially greater basicity of the hydrazine adduct than the azo starting material provides about 12–14 kcal/mol of exothermicity for cycloaddition of the protonated azo compound relative to that of the unprotonated azo compound, and we have called these “proton-driven” Diels–Alder reactions.² Although 1H^+ adds to 1,3-cyclopentadiene, 1,3-cyclohexadiene, and 1,3-cycloheptadiene, no addition product could be isolated for 2H^+ to 1,3-cyclopentadiene, which is reasonable on thermodynamic grounds. The addition reaction is expected to be endothermic even for the protonated azo compound in this case.³

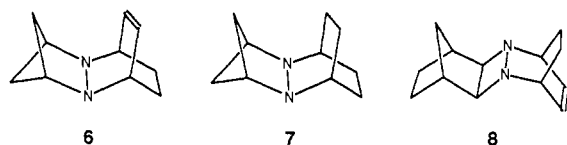
In this work the proton-driven Diels–Alder reaction is extended to the smaller CNN angle azo compounds **3** and **4** ($\alpha(\text{CNN})$ 95.5°



and 103.6° by modified MM1⁴ molecular mechanics calculations) and larger angle **5** ($\alpha(\text{CNN})$ 117.2° by MM1; for **1** and **2**, $\alpha(\text{CNN})$ is 107.6° and 114.0° by MM1 and 108.4° and 115.1° experimentally⁴). The product sesquibicyclic hydrazines provide a wider range for study of the effects of nitrogen pyramidalities upon electron loss and spectral properties.

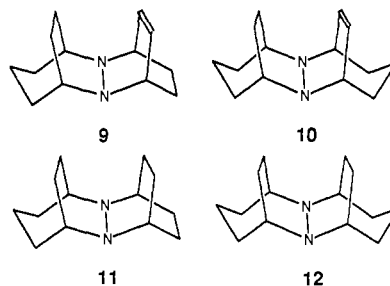
Results

Compound Preparation. Diels–Alder addition of 3H^+ and 4H^+ to cyclic dienes would give sesquibicyclic hydrazines with especially small CNN angles. Reactions in acetonitrile, the solvent used for previous work on 1H^+ and 2H^+ , gave rather rapid azo compound decomposition accompanied by gas evolution. The protonated forms of these rather strained azo compounds are unstable in acetonitrile, presumably because of $\text{R}_2\text{CH}-\text{N}$ bond cleavage, followed by loss of nitrogen. Rapid gas evolution upon protonation does not occur when **3** and **4** are reacted with $\text{HBF}_4 \cdot \text{Et}_2\text{O}$ in ether, which precipitates the protonated azo compound as a stable, white solid. Rapid addition of 1,3-cyclohexadiene to 4H^+ in acetonitrile gave protonated **6** in only a modest yield of 21%, but **6** proved

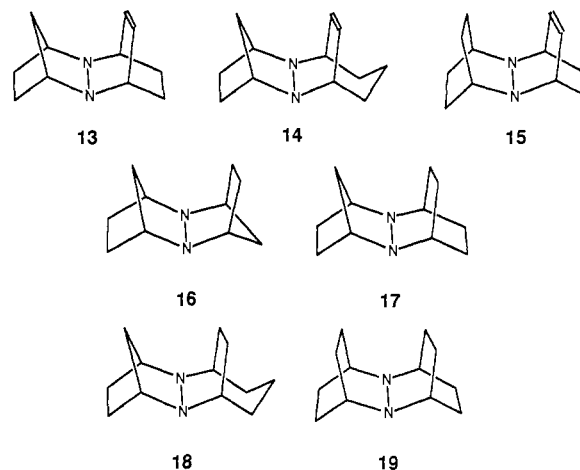


to be isolable. It failed to catalytically hydrogenate with Pd on BaSO_4 , K_2CO_3 , conditions which were successful for several other such adducts,^{1,2} but a 53% yield of the saturated hydrazine **7** resulted from diimide reduction. Although NMR peaks consistent with successful addition of 4H^+ to cyclopentadiene were initially observed, they disappeared rather rapidly, and we were never able to isolate an adduct from this reaction. In CH_2Cl_2 , 3H^+ and 1,3-cyclohexadiene gave protonated **8**, from which neutral **8** was isolated in 58% yield. We detected only one stereoisomer by ¹³C NMR and write the double-bond orientation and nitrogen stereochemistry shown because we expect this to be the stablest isomer and hence the one produced. Reduction of **8** was not attempted.

The 1,3-cyclohexadiene and 1,3-cycloheptadiene adducts of **5** were prepared in acetonitrile and reduced as previously reported for adducts of **2**, making **9–12** available. These sesquibicyclic

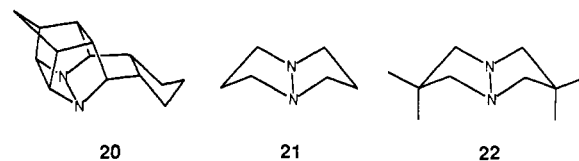


hydrazines should be flatter at nitrogen than the previously studied^{1–3} compounds **13–19**. We assign stereochemistry with



the double bond syn to the two-carbon bridge of the saturated bicyclo[3.2.2]nonyl rings for both **9** and **10** and the syn isomer for **12**. Only one isomer of each compound was detected by ¹³C NMR, and the isomers shown are expected to be the stablest ones. The proton NMR spectra of **9** and **10** were unfortunately too complex to allow us to prove our assignment of the protons shifted upfield by the unsaturation present as being on the two-carbon bridge on the other side of the nitrogens. The methylene carbon signals of **19** split into two sets when nitrogen inversion becomes slow on the NMR time scale (the coalescence temperature is -51°C).³ We did not observe the methylene carbons of **12** even begin to broaden at -90°C ,⁵ which is consistent with **12** being the syn isomer shown, and hence it is also consistent with the stereochemistry shown for **9** and **10**.

Berning and Hünig's⁶ internal 2 + 2 photolytic addition of a substituted norbornene to a bicyclo[2.2.2]octyl azo compound makes the lone pair, lone pair dihedral angle $\theta = 0^\circ$ cage diazetidene **20** available. Compound **20** is constrained to have even



more pyramidal nitrogens than diazetidene **8** and is significantly harder to oxidize.^{6b} We also will consider data for diazabicyclo[3.3.0]octane derivatives **21** and **22**, which have only monocyclic N,N' -fused rings and hence are not sesquibicyclic, but which have been shown by PE spectroscopy to have $\theta = 0^\circ$ conformations

(1) Nelsen, S. F.; Blackstock, S. C.; Frigo, T. B. *J. Am. Chem. Soc.* **1984**, *106*, 3366.

(2) Nelsen, S. F.; Blackstock, S. C.; Frigo, T. B. *Tetrahedron* **1986**, *42*, 1769.

(3) Nelsen, S. F.; Frigo, T. B.; Kim, Y.; Thompson-Colón, J. A.; Blackstock, S. C. *J. Am. Chem. Soc.* **1986**, *108*, 7926.

(4) Kao, J.; Huang, T.-N. *J. Am. Chem. Soc.* **1979**, *101*, 5546.

(5) We thank Mary Van Atten for carrying out this experiment. It is not known how much lower the barrier to double nitrogen inversion would be for **12**, so this experiment cannot be claimed to prove the stereochemistry suggested for it.

(6) (a) Berning, W.; Hünig, S. *Angew. Chem., Int. Ed. Engl.* **1977**, *16*, 777. (b) Nelsen, S. F.; Kessel, C. R.; Brace, H. N. *J. Am. Chem. Soc.* **1979**, *101*, 1874.

Table I. Cyclic Voltammetry Data for Sesquibicyclic Hydrazines^a

compd[code]	E°_1 [ΔE_p], V	E°_2 [ΔE_p], V	ref
Saturated Compounds			
20[Hun4]	+0.81 [0.07]	irr	6b
16[221/221]	+0.01 [0.10]	1.12 [0.17]	5b
7[211/222]	-0.02 [0.12]	1.06 [0.15]	this work
17[221/222]	-0.26 [0.07]	0.92 [0.08]	5b
18[221/322]	-0.22 [0.10]	1.01 [0.09]	5b
19[222/222]	-0.53 [0.07]	0.86 [0.07]	5b
11[222/322]	-0.55 [0.09]	0.98 [0.06]	this work
12[322/322]	-0.57 [0.09]	1.09 [0.10]	this work
21[5/5]	+0.08	irr	8
22[5/5M4]	-0.01	irr	8
Unsaturated Compounds			
8[4/u222]	+0.43 [0.09]	irr ^b 1.43	this work
6[211/u222]	+0.14 [0.07]	1.11 [0.13]	this work
13[221/u222]	+0.01 [0.08] ^c	0.95 [0.09]	5b
14[221/u322]	-0.04 [0.07]	1.04 [0.08]	5b
15[222/u222]	-0.25 [0.07]	0.95 [0.08]	5b
9[322/u222]	-0.27 [0.08]	1.00 [0.08]	this work
10[322/u322]	-0.37 [0.10]	1.12 [0.07]	this work

^a Room temperature, 1–2 mM hydrazine in acetonitrile containing 0.1 M tetrabutylammonium perchlorate, 0.2 V s⁻¹ scan rate, at a gold electrode, vs saturated calomel electrode. ^b Peak potential for an irreversible oxidation wave. ^c The +0.06 reported in ref 5b is in error.

comparable in energy to ones twisted at the NN bond.^{7,8}

Results and Discussion

Oxidation Thermodynamics. Cyclic voltammetry data for 6–22 are summarized in Table I, where the entries are listed in order of anticipated increasing flattening at N for saturated and unsaturated compounds separately. The “code” entry gives the ring sizes for the bicyclic rings fused at the nitrogens and is included for convenience in identifying the compounds. Photoelectron spectroscopic vertical ionization potential (vIP) values determined for sesquibicyclic hydrazines appear in Table II. The separation between the symmetric and antisymmetric lone pair dominated ionization bands (designated n₊ and n₋, and their separation $\Delta\text{IP}(n)$ in Table II) should be a maximum for planar nitrogens with $\theta = 0^\circ$, and the separations of 2.7 eV observed for 19 and 11 are the largest yet observed. The n₋ band overlaps badly with the C=C π ionization for 9, 13, and 15, precluding much accuracy in measuring either vIP, although $\Delta\text{IP}(n)$ is clearly smaller for the unsaturated compounds 15 and 9 than for their saturated analogues 19 and 11.

The relative ease of removing an electron from the neutral compound (n) to produce the cation radical (c) varies substantially among these compounds. The total range for adiabatic ionization in solution, measured by E°_1 (Table I), is 1.38 V (31.8 kcal/mol), and the range is 0.71 V for the 5- to 7-membered ring sesquibicyclic hydrazines. Similar ranges (1.32 and 0.81 eV) are observed for gas-phase vertical ionization potentials (Table II). The compounds with more pyramidal nitrogens are harder to oxidize, and we previously showed that a rough correlation exists between E°_1 and $\alpha(\text{av})$ calculated by molecular mechanics using Allinger's MM2 program for the hydrocarbons with both N atoms replaced by CH groups.² For the 5- to 7-membered ring sesquibicyclic compounds, a thermodynamically significant reversible second oxidation wave corresponding to conversion of c to the dication (d) is also observed. The range in reversible E°_2 values is 0.26 V, only 37% as large as the range in E°_1 for the corresponding compounds.

The effect of the geometry change which occurs upon electron removal on the energy of the system should be simpler to consider for sesquibicyclic hydrazines than for other types. The n forms of hydrazines typically have gauche N lone pairs, and their c forms have a substantial electronic preference for 180 or 0° lone pairs

Table II. Photoelectron Spectroscopic Data for Sesquibicyclic Hydrazines

compd[code]	vIP(n ₊) ^a	vIP(n ₋) ^a	$\Delta\text{IP}(n)$ ^a	vIP(π) ^a
Saturated Compounds				
20[Hun4]	7.63 ^b	—	—	—
16[221/221]	6.90	9.21	2.31	—
17[221/222]	6.81	9.11	2.30	—
19[222/222]	6.36	9.07	2.71	—
11[222/322]	6.31	9.04	2.73	—
12[322/322]	6.34	8.94	2.60	—
Unsaturated Compounds				
8[4/u222]	~7.3 ^c	—	—	~8.8 ^c
13[221/u222]	7.12	~9.3 ^d	~2.2	~8.9 ^d
14[221/u322]	6.84	8.72	1.88	9.26
15[222/u222]	6.72	~8.9 ^e	~2.2	~8.9 ^e
9[322/u222]	6.51	~8.7 ^f	~2.2	~8.7 ^f
10[322/u322]	6.50	8.69	2.19	9.16

^a Unit, electronvolts. Error estimated in numbers quoted to two places, 0.03 eV. ^b From ref 6b. ^c Very broadened spectrum. The first ionization region was fit with two Gaussians centered at 7.1 and 7.5 eV. There is absorption near 9.4 which could correspond to vIP(n₋), but no clear maximum was observed. ^d Complex region fit with Gaussians centered at 8.91, 9.26, and 9.64 eV. ^e Fit with Gaussians centered at 8.82 and 9.00 eV. ^f Fit with Gaussians centered at 8.66 and 8.83 eV.

because of the 3e- π bond present. Changes in θ and $d(\text{NN})$ upon electron removal significantly change nonbonded interactions between the alkyl groups on adjacent nitrogens in n and c. These effects are minimized in sesquibicyclic hydrazines, where θ is near 0° in both the n and c forms,⁹ and N,N' rings are present. The geometry change upon electron removal from 15 and 19 is substantial, roughly 10% shortening of the NN bond and 53% and 60% increments of the 10.5° $\alpha(\text{av})$ change between tetrahedral and planar nitrogens, respectively.⁹ In contrast to MNDO semiempirical molecular orbital calculations, which greatly overestimate nonbonded interactions and get almost all c forms as planar at N,⁹ the AM1 method¹⁰ obtains close to the x-ray $\alpha(\text{av})$ values for n and c forms of 15 and 19.³ AM1 calculations also predict about the observed enthalpy barrier to electron transfer between 19 and its cation radical,¹¹ suggesting that energy changes as well as nitrogen pyramidalities might be calculated usefully well.

In this work we have a wide enough range of structures to test the hypothesis that nitrogen pyramidalities is the dominant factor in determining how difficult it is to remove electrons from sesquibicyclic hydrazines. We use $\alpha(\text{av})$, the average of the three heavy atom bond angles at nitrogen, to describe the pyramidalities at nitrogen for reasons described below. Table III summarizes the $\alpha(\text{av})$ values and ΔH_f differences between n and c and between c and d (where the second electron removal is electrochemically reversible) obtained for geometry-optimized n, c, and d forms of the compounds of Table I, with the AM1 Hamiltonian and by employing unrestricted Hartree-Fock calculations (abbreviated AM1-UHF) for the open-shell c form. Figure 1 shows plots of calculated differences in ΔH_f for both oxidations versus $\alpha(\text{av})$ of the reduced form for the 5- and 7-membered ring sesquibicyclic compounds. The saturated (circles) and unsaturated (squares) compounds considered separately do not give significantly different correlation lines. The average vertical deviation from a regression line through both the saturated and unsaturated compound points for the first (n,c) electron transfer (shown in Figure 1a) is 0.05 eV (5% of the total range of $\Delta(\Delta H_f)$), and the slope of the line is -0.226, while the average deviation is 0.04 eV (5% of the total range) and the slope is -0.222 for the second (c,d) electron transfer (shown in Figure 1b). Despite a rather wide range in $\alpha(\text{av})$ values obtained by changing ring sizes at the nitrogen substituents, all of the effects going into producing the $\Delta(\Delta H_f)$ value to within

(9) Nelsen, S. F.; Blackstock, S. C.; Haller, K. J. *Tetrahedron* **1986**, *42*, 6101.

(7) (a) Nelsen, S. F.; Buschek, J. M. *J. Am. Chem. Soc.* **1974**, *96*, 6982, 6987. (b) Nelsen, S. F.; Rumack, D. T.; Meot-Ner, M. *J. Am. Chem. Soc.* **1988**, *110*, 7945.

(8) (a) Nelsen, S. F.; Peacock, V. E.; Weisman, G. R. *J. Am. Chem. Soc.* **1976**, *98*, 5269. (b) Nelsen, S. F.; Echevoyen, L. *Ibid.* **1975**, *97*, 4930.

(10) (a) Dewar, M. J. S.; Zoebisch, E. G.; Healy, E. F.; Stewart, J. J. P. *J. Am. Chem. Soc.* **1985**, *107*, 3902. (b) AM1 calculations used the AMPAC 1.00 package (*QPCE Bull* **1986**, *506*, 24a).

(11) Nelsen, S. F.; Blackstock, S. C.; Kim, Y. J. *J. Am. Chem. Soc.* **1987**, *109*, 677.

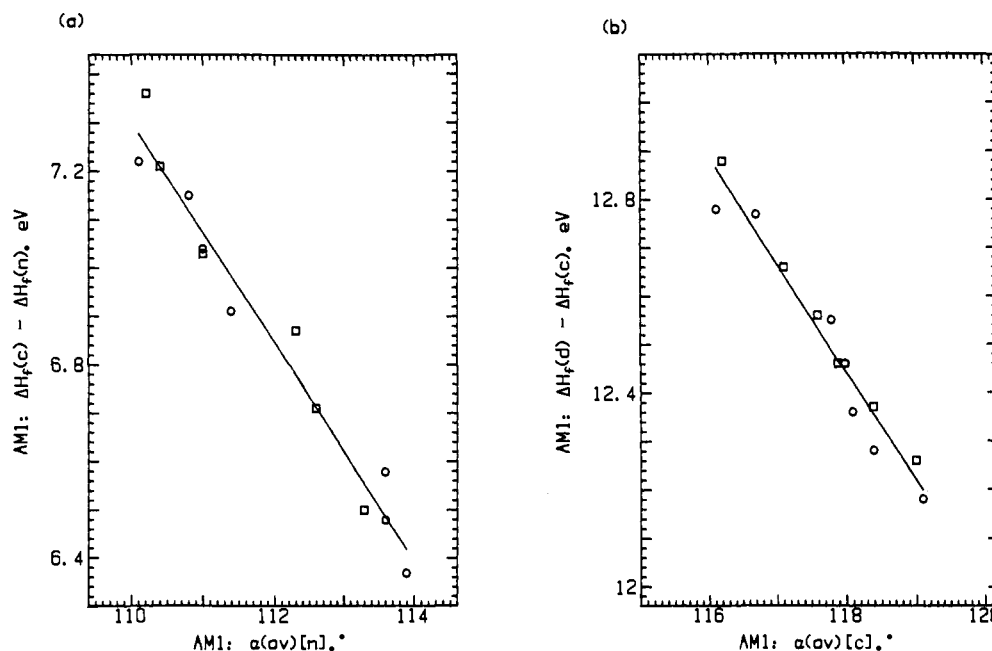


Figure 1. (a) Plot of AM1-calculated difference in c and n form heats of formation versus $\alpha(\text{av})$ of the n form for 5- and 7-membered ring sesquibicyclic hydrazines. Saturated compounds are shown as circles and unsaturated ones are shown as squares. (b) Plot done in the same way as part a for second electron loss, versus $\alpha(\text{av})$ of the c form.

Table III. Summary of AM1 Calculations^a on Sesquibicyclic Hydrazines

compd[code]	$\alpha(\text{av})$, deg		$\Delta(\Delta H_f)$, eV	
	n	c	n,c ^b	c,d ^c
Saturated Compounds				
20[Hun4]	102.5	105.3	8.21	
16[221/221]	110.1	116.0	7.22	12.78
7[211/222]	110.8	116.5	7.15	12.77
17[221/222]	111.0	117.5	7.04	12.55
18[221/322]	111.4	117.7	6.91	12.46
19[222/222]	113.6 ^d	118.1 ^d	6.58	12.36
11[222/322]	113.6	119.0	6.48	12.28
12[322/322]	113.9	119.6	6.35	12.19
21[5/5]	111.1	117.7	7.25	
22[5/5M4]	111.1	117.7	7.08	
Unsaturated Compounds				
2[4/u222]	106.1	114.7	7.50	
6[211/u222]	110.2	116.2	7.36	12.88
13[221/u222]	110.4	117.2	7.21	12.66
14[221/u322]	111.0	117.7	7.03	12.56
15[222/u222]	112.3 ^e	118.0 ^e	6.87	12.46
9[322/u222]	112.6	118.5	6.71	12.37
10[322/u322]	113.3	118.9	6.50	12.26

^a AM1-UHF geometry optimization was used for c. ^b Difference in heats of formation for c and n. ^c Difference in heats of formation for d and c. ^d X-ray crystallographic $\alpha(\text{av})$ for n = 112.1°; for c $\alpha(\text{av})$ = 117.7°. ^e X-ray crystallographic $\alpha(\text{av})$ for n = 112.8°; for c $\alpha(\text{av})$ = 118.3°.

5% of its actual value in these calculations are contained in the pyramidality at nitrogen, as measured by the *single parameter* $\alpha(\text{av})$. We consider this to be a striking result. The minimum geometric information necessary to define pyramidality at nitrogen is twelve *x, y, z* coordinates (or six internal coordinates of distance, angle, and dihedral angle) to describe the relative positions of the nitrogens and their α carbons for a hydrazine with equivalent nitrogens. Furthermore, the details of the constitution of the sigma framework leading to those atoms occupying the positions that they do could have been significant in determining the ease of electron removal. This result of the ease of oxidation being properly described by only using $\alpha(\text{av})$ does not occur with classes of hydrazines other than sesquibicyclic ones.

The next question we consider is whether the AM1 prediction of $\alpha(\text{av})$ providing a one-parameter measurement of the ease of electron loss from sesquibicyclic hydrazines is consistent with

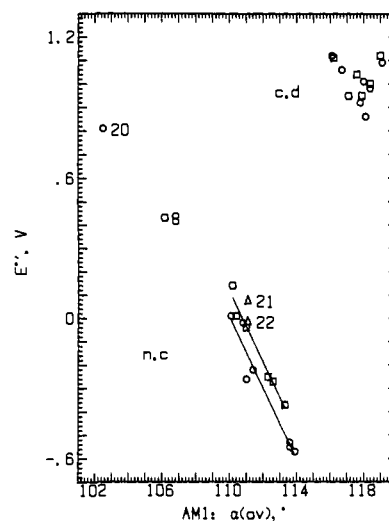


Figure 2. Plot of $E^{\circ'}$ versus $\alpha(\text{av})$ of the lower oxidation state for both the n,c and c,d electron transfers. Saturated sesquibicyclic compounds are shown as circles and unsaturated ones are shown as squares. Points for the bicyclo[3.3.0]octyl derivatives **21** and **22** are included as triangles.

experiment. AM1 calculations do not give the correct size for ionization potentials of sesquibicyclic hydrazines. The calculated values of $v\text{IP}$ assuming Koopmans theorem, $\Delta H_f(\text{cng}) - \Delta H_f(\text{n})$ [where *cng* indicates the cation in the geometry of the neutral compound], for the compounds of Table II are 1.00–0.71 eV higher than the observed $v\text{IP}(\text{n}^+)$ values, and the difference for the saturated compounds decreases as the bridge sizes increase (**20**–[hun4], 0.97 eV; **16**[221/221], 1.00; **17**[221/222], 0.94; **19**–[222/222], 0.88; **11**[222/322], 0.86; **12**[322/322], 0.75). The differences between calculated and observed $v\text{IP}$ for the unsaturated compounds are less regular and show no better agreement with experiment. The changes calculated for the thermodynamics of electron removal in solution as the ring sizes are changed are much more successful. Figure 2 shows a plot of the experimental $E^{\circ'}$ data of Table I versus the AM1 $\alpha(\text{av})$ value for the reduced form. The most obvious feature of Figure 2 is that $E^{\circ'}$ for the n,c electron transfer gives a good correlation with $\alpha(\text{av})[\text{n}]$, as expected from Figure 1a, but that there is no correlation of $E^{\circ'}$ for the c,d electron transfer with $\alpha(\text{av})[\text{c}]$, despite Figure 1b. We shall discuss the n,c electron transfer first. The saturated (circles)

Table IV. Comparison of Estimated n,c Enthalpy Differences Obtained from E° by Adjusting for Solvation Energy Differences with Values Calculated with AM1^a

compd[code]	$\sum n(\text{eff})$	$E^{\circ,b}$	$\Delta(\Delta G^{\circ}s)^c$	$\Delta(\Delta H[e])^d$	$\Delta(\Delta H_f)[n,c]^e$
16 [221/221]	9.74	0.54	-0.09 ₈	+0.64	+0.64
7[211/222]	9.74	0.51	-0.09 ₈	+0.61	+0.57
17[221/222]	10.61	0.27	-0.04 ₆	+0.32	+0.46
18 [211/322]	11.09	0.31	-0.02 ₂	+0.33	+0.33
19 [222/222]	11.48	[≡0]	[≡0]	[≡0]	[≡0]
11 [222/322]	11.96	-0.02	+0.02 ₇	-0.05	-0.10
12 [322/322]	12.44	-0.04	+0.05 ₇	-0.10	-0.21

^aAll energies are given in electronvolts, relative to **19**[222/222]. ^b E°_1 (observed)- E°_1 (**19**). ^cFrom eq 2. ^dFrom eq 1. ^eCalculated by AM1.

and unsaturated (squares 5- to 7-membered ring sesquibicyclic hydrazines give the correlation lines shown, which are nearly parallel (the vertical separation between the lines is $0.10_7 \pm 0.00_3$ V between $\alpha(\text{av})$ of 110.2° and 113.3°). The compounds which fall farthest from the regression lines for the saturated and unsaturated compounds deviate in the same directions: **7**[211/222] is 0.10 V harder to oxidize than the line predicts and **6**[211/u222] is 0.05 V harder, while **17**[221/222] is 0.11 V easier to oxidize than the line predicts and **13**[221/u222] is 0.05 V easier. Despite these larger deviations, the correlation of E°_1 with $\alpha(\text{av})$ is about as good as the correlation of calculated $\Delta(\Delta H_f)$ with $\alpha(\text{av})$ for these compounds noted above. The average deviation of observed E°_1 from the line shown for the saturated compounds is 0.04_0 V, and that for the unsaturated compounds is 0.02_4 V, which is comparable to the average deviation of 0.05 eV for the calculated ΔH_f change. Experimental error in E°_1 determination is about 0.01 V.

In principle, several factors make changes in E° different from those in $\Delta(\Delta H_f)$. E° values represent free energy, not enthalpy changes. Although ΔS° values for gas phase electron transfer equilibria do vary significantly for tetraalkylhydrazines with different substituents,^{7b} we would expect sesquibicyclic hydrazines to show similar entropies, which would tend to make E° changes parallel those in $\Delta(\Delta H_f)$ well. The most important difference between E°_1 and $\Delta(\Delta H_f)[n,c]$ for these compounds is likely to be solvation energies; E°_1 must contain any differences in solvent stabilization of n and c as the alkyl groups are changed, while the calculations cannot. Obtaining a straight lines for E°_1 vs $\alpha(\text{av})$ in Figure 2 requires not only that the inherent ease of electron removal correlate with $\alpha(\text{av})$, as predicted in Figure 1a, but also that changes in solvation energy as the alkyl groups are changed are regular with $\alpha(\text{av})$. We believe that the reason for obtaining straight lines is not that solvation energy differences between the sesquibicyclic hydrazines studied are negligible but that they change regularly with the size of the alkyl groups. High-pressure mass spectrometry measurements have recently determined how solvation energies for n,c equilibria of 30 saturated tetraalkylhydrazines change with alkyl-group structure,^{7b} although volatility allowed only one sesquibicyclic compound, **16**[221/221], to be included in the data set. Solvent stabilization for the n,c equilibrium (presumably predominately for the charged c form) decreases as the alkyl groups are enlarged. Solvent stabilization is largest for Me_2NNMe_2 and 7.1 kcal/mol smaller for **16**. What we had not anticipated is that the measured change in solvation energy as alkyl groups are enlarged, $\Delta(\Delta G^{\circ}s)$, correlates linearly with the sum of the gas-phase alkyl group "inductive" parameters, $n(\text{eff})$, for the attached alkyl groups. Quantitatively, the regression line for the compounds studied^{7b} had a slope of $0.056 \text{ eV}/n(\text{eff})$ unit.¹² In Table IV we list $\sum n(\text{eff})$ values and compare the observed changes in E° relative to **19**[222/222] with the estimated changes in solvation energy, $\Delta(\Delta G^{\circ}s)$ and the resulting estimated changes in enthalpy for electron transfer, which we shall abbreviate as $\Delta(\Delta H[e])$, calculated as shown in eq 1 and 2 with $\Delta(\Delta H_f)[n,c]$

$$\Delta(\Delta H[e]) = E^{\circ} - E^{\circ}(\mathbf{19}) - \Delta(\Delta G^{\circ}s) \quad (1)$$

$$\Delta(\Delta G^{\circ}s) = 0.056(\sum n(\text{eff}) - 11.48) \quad (2)$$

values calculated by AM1 (Table I). It will be noted that the solvation energy corrections are estimated from eq 2 to be significant, covering a range of 0.16 V for the saturated compounds of Table I. When the solvation energy adjustment of eq 1 and 2 is made, the $\Delta(\Delta H[e])$ difference obtained for **16** relative to **19** from the difference in E°_1 values is the same size as the $\Delta(\Delta H_f)[n,c]$ difference calculated by AM1. The slope of an E°_1 versus $\Delta(\Delta H_f)[n,c]$ plot (not shown) is 0.70 without the solvation energy correction. The solvation energy correction improves agreement for (but does not totally eliminate) the anomalously low E°_1 value for **17**[221/222]. We conclude that at least part of the reason that **17** is easier to oxidize than **18**[221/322] is the difference in their solvation energies. We note that, at the less pyramidal end of the sesquibicyclic hydrazine series, **11**[222/322] and **12**[322/322] are not as easy to oxidize relative to **19**[222/222] as AM1 predicts them to be, even after the solvation energy adjustment. AM1 calculations fail to get lower energies for forms of bis-N,N'-cycloalkylhydrazines which are experimentally known to be twisted, such as the only slightly twisted **19** and even 1,5-diazabicyclo[3.3.0]octane **21**, which is substantially twisted in its stablest form, although PE spectroscopy has shown that the energy of the $\theta = 0^\circ$ form is not very much higher because both conformations can be observed.^{7b} The calculations quoted were done without twist in the bicycloalkyl groups in all cases, because AM1 gets these as the minimum-energy structures for the cases tested anyway. There may well be a problem with the AM1 calculations for larger ring size sesquibicyclic compounds, where twisting about the NN bond of n presumably would occur to relieve lone pair, lone pair interaction. The smaller $\Delta\text{IP}(n)$ observed in the PE spectrum of **12**[322/322] than for that of **11**[222/322] and the similar size of $\Delta\text{IP}(n)$ for **11** and **19**[222/222] are consistent with the introduction of $(\text{CH}_2)_3$ bridges allowing more twisting.

Figure 2 also contains E° data on some compounds other than the 5- to 7-membered ring sesquibicyclic ones discussed above. Experimentally, E°_1 is lower for the small $\alpha(\text{av})$ diazetidines **8** and **20** than predicted from a line through less constrained compounds, their points lying below extrapolations of the lines shown for the larger ring compounds by 0.28 and 0.33 V, respectively. Deviations from linearity in plots of energy-related quantities over large enough spans of $\alpha(\text{av})$ are predicted. For example, a plot of the calculated negative of the HOMO energy ($-E$) versus $\alpha(\text{av})$ for ammonia (not shown) curves slightly, and $-E$ is calculated to be 0.09 eV higher at 102° than a regression line through the 120° - 116° points.

Observing nearly parallel correlation lines displaced by 0.1 V for the unsaturated and saturated compounds in Figure 2, but no significant difference between the two classes of compounds in Figure 1a suggests either that the more difficult oxidation of unsaturated hydrazines is not really an "inductive" effect as we have called it in the past³ but a solvent effect or that AM1 calculations are poor at handling the effects of allylic unsaturation; both statements may be true. We note that a 0.1 V increase in E°_1 is observed for monocyclic allylic hydrazines which lack steric interactions between the alkyl groups.³ This increase is consistent with a substantial solvation energy component to the observed increase in E°_1 for unsaturated compared to saturated hydrazines.

We now consider the c,d electron transfer step, which experimentally shows no correlation with $\alpha(\text{av})$ (see Figure 2). We believe that the calculated similar slopes and correlations in Figure 1 for n,c and c,d electron transfer enthalpies make it overwhelmingly likely that the principal cause of a lack of correlation for E°_2 with $\alpha(\text{av})$ is changes in the solvation energy of d as the alkyl groups are changed. We have previously pointed out rather clear examples of dication solvation energy change effects on E°_2 for syn and anti isomers 8,8'-bis-8-azabicyclo[3.2.1]octane¹² and for N,N-bicyclic tetraalkyltetraene dications.¹³ We believe it is worth repeating here that the linear correlation observed^{7b} for solvation energy changes [$\Delta(\Delta G^{\circ}s)$] with alkyl group "inductive" effect [$\sum n(\text{eff})$] for c is consistent with its solvation principally

(12) Nelsen, S. F.; Blackstock, S. C.; Steffek, D. J.; Cunkle, G. T.; Kurtzweil, M. L. *J. Am. Chem. Soc.* **1988**, *110*, 6149.

(13) Nelsen, S. F.; Cunkle, G. T.; Evans, D. H.; Haller, K. J.; Kaftory, M.; Kirste, B.; Clark, T. *J. Am. Chem. Soc.* **1985**, *107*, 3825.

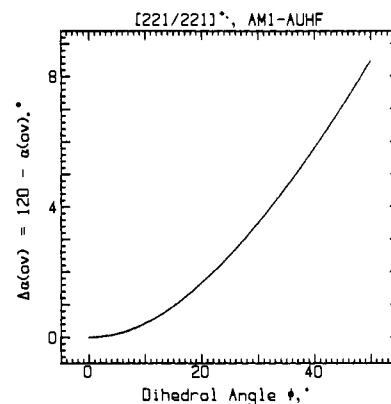
Table V. ESR Nitrogen Splitting Constants of Sesquibicyclic Hydrazine Cation Radicals and N(2s) Spin Densities Calculated for the Optimized Structure

compd[code]	solv	T, °C	a(N), G	ref	10 ³ ρ(N) from AM1 ^a
Saturated Compounds					
20[Hun4]	PrCN	-90	26.8	6b	56.2
16[221/221] ^b	PrCN	23	20.8	3	43.2
7[211/222] ^c	CH ₂ Cl ₂	23	20.6	this work	41.4
17[221/222]	CH ₂ Cl ₂	-75	16.1	3	40.5
18[221/322]	PrCN	23	14.4	this work	37.3
19[222/222] ^d	PrCN	22	15.1	1	37.4
11[222/322]	MeCN	23	13.9	this work	35.5
12[322/322]	PrCN	23	13.0	this work	20.3 ^e
21[5/5]	MeCN	23	17.6	8b	41.0
22[5/5M4]	PrCN	23	17.1	8b	43.4
Unsaturated Compounds					
8[4/u222]	PrCN	14	21.5	this work	39.8
6[211/u222]	PrCN	-80	21.9	this work	45.5
13[221/u222]	CH ₂ Cl ₂	-80	17.2	3	44.0
14[221/u322]	MeCN	23	15.2	this work	42.2
15[222/u222]	MeCN	23	19.2	1	40.5
9[322/u222]	MeCN	23	16.0	this work	37.1
10[322/u322]	PrCN	23	13.5	this work	30.7

^a Calculated for geometry-optimized structure by AM1-UHFQ. ^b A decrease of 1.8 mG/deg of $a(2N)$ is observed when the temperature is raised between -85 and 22 °C for **16**- d_{12} . ^c See the text for a discussion of the temperature effect. ^d A decrease of 3.7 mG/deg of $a(2N)$ is observed when the temperature is raised between -85 and 22 °C. ^e A value of 27.5 is calculated for the energy minimum with the two-carbon bridges syn.

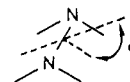
involving interactions with the alkyl groups. Charge distributions for **c** calculated by AM1 are consistent with this. The nitrogens remain negatively charged in **c**, and all of the positive charge is calculated to be on the hydrogens. For the **d** forms, AM1 calculations do get positively charged nitrogen atoms, and the accessibility of these nitrogens to counterion and solvent changes substantially as bicyclic ring sizes are changed. Smaller bicyclic rings make the nitrogens more accessible, but lower $\sum n(\text{eff})$. These opposing effects presumably contribute to the observed lower E°_2 values for compounds in the middle range of $\alpha(\text{av})$ values of Table I.

Nitrogen ESR Splitting Constants. The nitrogen splitting constant, $a(N)$, in the ESR spectrum of tetraalkylhydrazine cation radicals is sensitive to pyramidalization at nitrogen. Despite formally identical total spin densities at nitrogen of 0.5, $a(N)$ varies from 13.0 to 26.8 G for the compounds discussed here. Hydrazine cation radicals which are planar at nitrogen would have a pure p singly occupied NN π^* MO and a minimum nitrogen splitting. Syn bending at nitrogen, as is present in sesquibicyclic hydrazines, gives larger $a(N)$ values than the anti bending present in less constrained hydrazine cation radicals because of symmetry effects.¹⁴ Increasing syn bending causes the singly occupied NN π^* orbital to mix more with a low-lying NN, NC_α combination σ^* orbital, increasing the σ character of the singly occupied MO, which increases $a(N)$. These effects are predicted by both ab initio and semiempirical MNDO calculations as **H**₂NNH₂²⁺ is pyramidalized and is experimentally observed in experimental $a(N)$ values for syn and anti bent tetraalkylhydrazines where different amounts of bending were enforced by including the hydrazine unit in N,N and N,N' rings.¹⁴ The nitrogen splittings observed for **6**-**22** appear in Table V, in which it is clear that more pyramidal compounds show larger $a(N)$. For **10**²⁺ and **12**²⁺, where both bicyclic rings are 6,7-diazabicyclo[3.2.2]nonyl systems, nitrogen splittings no larger than that of tetramethylhydrazine cation radical are observed, indicating quite planar or possibly anti-pyramidalized structures. The ESR spectra of **16**²⁺[221/221] and of **7**²⁺[211/222] are notably similar both in size and temperature dependence of the nitrogen splitting and in the double nitrogen

**Figure 3.** Plot of $\Delta\alpha(\text{av})$ versus ϕ for **16**²⁺

inversion barrier measured by variable temperature ESR experiments. Simulations of the VT-ESR spectrum of **16**²⁺- d_{12} gave $\Delta G^{\ddagger}(-85\text{ °C})$ of 4.6 kcal/mol, as described previously.³ The presence of the bicyclo[2.1.1]hexyl ring in **7** places the anti hydrogens in the one carbon bridges in the plane of the node between the nitrogens in the HOMO, causing significantly less broadening by proton splittings than in the spectrum of unlabeled **16**²⁺. We were able to simulate low temperature spectra of **7**²⁺ using $a(2H) = 6.1$, $a(2H) = 2.1$ G for the "frozen" spectrum, corresponding to W-plan aligned and nonaligned anti hydrogens in the two-carbon bridges of the bicyclooctyl unit. Best fit simulations of dynamically averaging spectra recorded at -83 °C with $a(N) 21.05$ G, line width of 1.3 G, and at -102 °C with $a(N) 21.08$ G, line width of 1.5 G, gave double nitrogen inversion rates of 1.7×10^7 and 4.4×10^6 s⁻¹, respectively, corresponding to inversion barriers of 4.6 kcal/mol. Although these numbers are not as accurate as those determined for **16**²⁺- d_{12} , it is clear that the double nitrogen inversion barrier, as well as the size of nitrogen splitting constant and its temperature dependence, are very similar for these two compounds. We shall not report or discuss the proton splittings for the other compounds here because ESR experiments do not give very good resolution for these compounds and no additional information about nitrogen pyramidalization would result. The magnitude of W-plan hydrogen splittings, although sensitive to bending at nitrogen, cannot yet be quantitatively related to it.³

The nitrogen ESR splitting constant $a(N)$ should be directly proportional to the nitrogen 2s spin density, $\rho(N)$, and a comparison of $a(N)$ with calculated $\rho(N)$ should provide an unusually direct check upon the utility of the calculations for rationalizing pyramidalization effects. Because internal coordinates are used to input structures for calculations, pyramidalization at nitrogen can be changed by varying the dihedral angle between the two CNNC planes, ϕ or its equivalent. The plot of $\Delta\alpha(\text{av}) = 120 - \alpha(\text{av})$ versus



ϕ (see Figure 3) shows that these two criteria for pyramidalization are far from being linear with each other. The slope approaches zero at small ϕ values but rises to 0.27 at $\phi = 50^\circ$. Similar curves are obtained for other sesquibicyclic hydrazines. Use of ϕ as the criterion for pyramidalization instead of $\alpha(\text{av})$ significantly alters the shape of calculated ΔH_f versus bending curves in the region near planar nitrogen atoms, and we use $\Delta\alpha(\text{av})$ as the criterion for nitrogen pyramidalization throughout this work.

The wave functions obtained using AM1-UHF are slightly spin contaminated, having (S^2) values of 0.755-0.758. Although the (S^2) increase is only about 1% over the value for a pure doublet of exactly 0.75, this modest amount of spin contamination is significant for consideration of the effects of pyramidalization on $a(N)$. The spin contamination is essentially all quartet, because the quartet annihilation method of Amos and Snyder,¹⁵ first

(14) Nelsen, S. F.; Blackstock, S. C.; Yumibe, N. P.; Frigo, T. B.; Carpenter, J. E.; Weinhold, F. *J. Am. Chem. Soc.* **1985**, *107*, 143.

(15) Amos, T.; Snyder, L. C. *J. Chem. Phys.* **1964**, *41*, 1773.

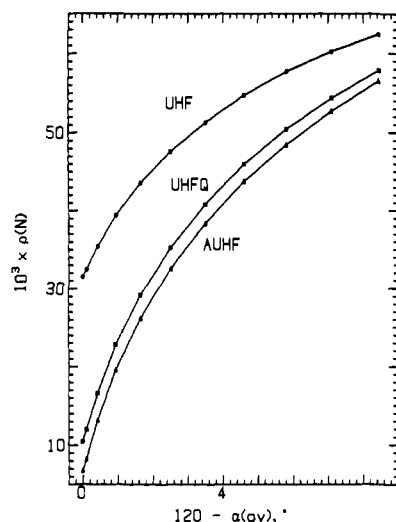


Figure 4. Comparison of nitrogen s-orbital spin densities as a function of nitrogen pyramidal angle calculated for 16^{*+} with AM1-UHF, after quartet annihilation (UHFQ), and with quartet annihilation after every SCF cycle so the geometry is optimized without quartet contamination (AUHF).

implemented in semiempirical calculations by Bischof,¹⁶ lowers (S^2) to under 0.75003. In these spin density calculations, called UHFQ here, quartet components are removed from the final wave function after the energy is optimized by UHF, which only adds seconds of CPU time to the calculation. Use of UHFQ significantly changes the shape of plots of calculated $\rho(n)$ versus $\Delta\alpha(av)$, as illustrated for $16[221/221]$ in Figure 4, where calculations carried out at 5° increments in ϕ are shown. It will be noted that the calculated ratio of UHF to UHFQ $\rho(N)$ changes significantly with pyramidal angle, dropping from 3.00 at $\Delta\alpha(av)$ of 0° to 1.08 at 8.46° , which would substantially change the expected value for $a(N)$ when averaging over an energy surface. We also examined a more accurate way of eliminating spin contamination, in which quartet components are annihilated after each SCF cycle, so the geometry optimization is carried out without quartet contamination, which we refer to as AUHF calculations. Use of AUHF results in a slightly higher calculated energy because of spin contamination in the states calculated by UHF, but this lowering in energy caused by spin contamination proves not to change significantly with pyramidal angle at N. For 16^{*+} the UHF energy is 0.67 kcal/mol higher than the AUHF energy at $\Delta\alpha(av) = 0$, drops to 0.52 kcal/mol higher at the energy minimum, and to 0.41 kcal/mol higher at $\Delta\alpha(av)$ of 8.46° . Similar calculated results were obtained for other hydrazine cation radicals. Although the AUHF $\rho(N)$ values are somewhat lower, the difference from UHFQ does not change significantly with pyramidal angle (see Figure 4) so no significant change in the calculated result would be obtained by using AUHF rather than UHFQ calculations. Because AUHF calculations take approximately 10 times as long to carry out, we have not felt the additional expense of using them justified the time which would be required, and UHFQ calculations have been employed for the rest of the compounds in this work.

The series examined allows consideration of whether the ring sizes of the alkyl groups are important in determining $a(N)$ by any effect other than changing nitrogen pyramidal angle. Because the increase in nitrogen splitting is caused by σ, π mixing, specific orbital interactions which vary with ring size and nodal properties of the alkyl group σ orbitals might well make the identity of the alkyl groups important. Figure 5 shows plots of nitrogen 2s spin density calculated by AM1-UHFQ versus pyramidal angle for the cations from $19[222/222]$, $7[211/222]$, and $16[221/221]$. It will be noted that $\rho(N)$ is calculated to be the same when the nitrogens are planar and N-N, C-N combination orbital mixing is symmetry

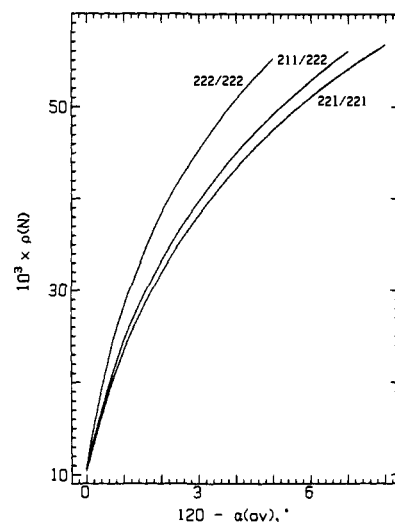


Figure 5. AM1-UHFQ nitrogen spin density as a function of bending at nitrogen for the cations from $19[222/222]$, $7[211/222]$, and $16[221/221]$.

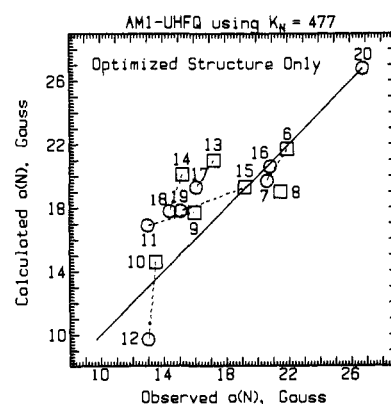


Figure 6. Plot of calculated versus observed $a(N)$ values for sesquibicyclic hydrazines using minimum-energy structures only and $K_N = 477$ G. Circles represent saturated compounds, and squares represent unsaturated ones. Compounds of the same sesquibicyclic ring sizes are connected by broken lines.

forbidden but that the curves differ as bending at nitrogen increases; $\rho(N)$ becoming significantly higher for the all two-carbon-bridged compound 19^{*+} than for its analogues with two methylene bridges. The difference between 19^{*+} and 16^{*+} is 21% at the $\Delta\alpha(av)$ value of 1.9° corresponding to the energy minimum for 19^{*+} , and 18% at the 3.9° corresponding to the energy minimum for 16^{*+} , while the curves are much closer for 7^{*+} and 16^{*+} , differing by about 4%. Similar results are obtained for the other compounds studied. In contrast to the calculated adiabatic energies for electron loss shown in Figure 1, which were not very sensitive to alkyl group structure, $\rho(N)$ is calculated to depend more upon alkyl group structure, and a single $\rho(N)$ versus $\Delta\alpha(av)$ curve should not be used for sesquibicyclic hydrazines.

The AM1-UHFQ $\rho(N)$ values obtained for the geometry-optimized structures (last column of Table V) do show some relation to observed $a(N)$ values. If the calculations worked perfectly, a simple proportionality constant K_N would convert $\rho(N)$ values to $a(N)$ values. We have elected to calibrate K_N for these sesquibicyclic hydrazines by using 477 G, the value which converts the calculated $\rho(N)$ for Hünig's cage compound 20^{*+} to the observed $a(N)$ value of 26.8 G. Compound 20^{*+} must have an unusually rigid structure compared to those for typical hydrazine cation radicals, because it can only change nitrogen pyramidal angle by changing σ bond lengths. We doubt that the AM1 calculation can have the structure very far off because of this rigidity. Comfortingly, 477 G is within the range of $a(N)/\rho(N)$ values obtained for less-constrained compounds. It is also not very far from the original value of 379.34 G taken by Pople and co-workers

(16) (a) Bischof, P. *J. Am. Chem. Soc.* **1976**, *98*, 6844. (b) Bischof, P.; Friedrich, G. *J. Comp. Chem.* **1982**, *3*, 486.

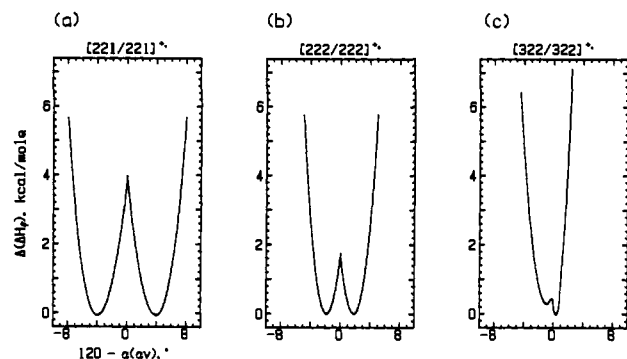


Figure 7. AM1-UHF-calculated energy versus $\Delta\alpha(\text{av})$ curves for the cations from **16**[221/221], **19**[222/222], and **12**[322/322].

from INDO calculations employing standard geometries.¹⁷ We show a plot of calculated versus experimental $a(\text{N})$ for AM1-UHF geometry-optimized structures as Figure 6, along with a line of slope 1 through the point for **20**⁺⁺, which was used to determine K_{N} . Saturated and unsaturated compounds of the same sesquibicyclic ring sizes are connected by broken lines. Agreement between the calculated and observed $a(\text{N})$ values is not very good.

Observed ESR splittings are time averages, and the energy surfaces for radicals are often shallow enough that the single minimum-energy structure does not properly represent the structure for the purpose of estimating ESR splittings. We recently discussed using AM1-calculated C-C bond rotational surfaces for rationalization of ESR data for simple saturated alkyl radicals.¹⁸ Because sesquibicyclic hydrazine pyramidalization appears to be usefully described as one dimensional in $\alpha(\text{av})$, we have examined the possibility of using the calculated energy surfaces to more fully understand the experimental $a(\text{N})$ data. Energy surfaces for the sesquibicyclic hydrazine cation radicals studied were calculated by optimizing the structure at 5° increments in ϕ between planar nitrogen atoms ($\phi = 0^\circ$) and pyramidalized geometries which were several kcal/mol higher in energy than the optimum. P. J. Certain and J. M. Standard carried out quantum mechanical calculations on these one dimensional energy surfaces, obtaining numerical wave functions which would produce the surface and calculating bound-state eigenvalues and expectation values for $\rho(\text{N})$ assuming the values calculated by AM1 and using moments of inertia calculated from the AM1 atom positions. The results obtained by these time-consuming and laborious numerical integrations, averaging over many dozens of states, was shown to produce the same answers as the computationally trivially simple classical Boltzmann averaging over the potential energy surface using eq 3 and 4. This result is not

$$\langle \rho(\text{N}) \rangle = \sum_i f(\Delta\alpha_i) \times \rho(\text{N})(\Delta\alpha_i) \quad (3)$$

$$\text{where } f(\Delta\alpha_i) = \frac{\exp[-\Delta(\Delta H_f(\Delta\alpha_i))/RT]}{\sum_i \exp[-\Delta(\Delta H_f(\Delta\alpha_i))/RT]} \quad (4)$$

surprising, as Krusic and co-workers have previously demonstrated similar agreement between quantum mechanical and classical solutions to one dimensional energy surfaces for bond rotation calculated for simple alkyl radicals.¹⁹ We found that smooth curves interpolated between the approximately 18–25 calculated points, with 0.1° increments in $\Delta\alpha(\text{av})$ provided enough points to give the same answers as the full quantum mechanical treatment for barriers to double nitrogen inversion down to 0.5 kcal/mol.

The energy surfaces calculated for sesquibicyclic hydrazines differ substantially as the rings are enlarged, as illustrated by the comparison of the AM1-UHF $\Delta(\Delta H_f)$ vs $\Delta\alpha(\text{av})$ plots for **16**⁺⁺[221/221], **19**⁺⁺[222/222], and **12**⁺⁺[322/322] shown in

Table VI. Averaged Nitrogen 2s Spin Densities for Cation Radicals Estimated by Averaging over AM1-UHF Energy Surfaces

compd-[code]	$\Delta H(\text{inv})^a$, kcal/mol	$\Delta\alpha(\text{av})$, deg (opt.) ^b	2nd ^c min	$10^3 \langle \rho(\text{N}) \rangle^d$	T coeff ^e $10^6 \rho(\text{N})/^\circ\text{C}$
Saturated Compounds					
16 [221/221]	3.8	± 4.0	(=0)	42.3	-2.7
{(AUHF)} ^f	4.0	± 4.0	(=0)	40.0	-2.9]
7 [211/222]	3.6	± 3.5	(=0)	41.8	-2.7
17 [221/222]	2.5	+2.5	0.1 [-2.2]	38.9	-3.3
18 [221/322]	1.7	-2.3	0.6 [+1.0]	38.4	-6.0
19 [222/222]	1.7	± 1.9	(=0)	36.0	-2.3
11 [222/322]	1.2	+1.1	0.3 [-1.5]	33.0	1.6
12 [322/322]	0.5	+0.4	0.3 [-0.9]	26.3	12.3
21 [5/5]	2.2	± 2.2	(=0)	42.2	-1.2
22 [5/5m4]	2.2	± 2.3	(=0)	42.4	-1.5
Unsaturated Compounds					
8 [4/u222]	3.7	-5.3	1.9 [+1.8]	38.6	-4.5
6 [211/u222]	4.0	-3.8	0.6 [+3.5]	44.0	-3.8
13 [221/u222]	3.0	-2.8	0.8 [+2.2]	42.1	-7.8
14 [221/u322]	2.2	-2.3	1.4 [+1.0]	40.1	-6.2
15 [222/u222]	2.1	-2.0	0.5 [+1.9]	38.6	-2.9
9 [322/u322]	1.5	-1.5	0.5 [+1.1]	35.3	-1.8
10 [322/u322]	0.5	-1.1	0.2 [+0.3]	29.4	4.5

^a From minimum-energy conformation to double nitrogen inversion maximum. ^b Negative $\Delta\alpha(\text{av})$ is used for the conformation shown for the neutral compounds in the structural drawings in the text, positive values are for its double nitrogen inversion isomer. ^c From minimum-energy conformation to the second minimum after double nitrogen inversion. The number in brackets is $\Delta\alpha(\text{av})$ calculated for this second minimum. ^d Averaged $10^3 \rho(\text{N})$ calculated at 25 °C using the AM1-UHFQ energy surface. ^e Temperature dependence of nitrogen spin density calculated between -78 and 25 °C. ^f Calculated with spin annihilation after every SCF cycle; see the text.

Figure 7. As the rings are enlarged, increasing the size of nonbonded interactions, the compounds become flatter, with lower double nitrogen inversion barriers, and the wells become narrower. We note that the energy surfaces obtained are roughly intersecting parabolas, of different widths and relative energies for unsymmetrical compounds like **12**⁺⁺. Negative $\Delta\alpha(\text{av})$ has been used for the conformation shown in the structural drawings, which has the two carbon bridges syn for **12**⁺⁺. The negative $\Delta\alpha(\text{av})$ energy well for **12**⁺⁺ is broader but 0.3 kcal/mol higher at its energy minimum than the positive $\Delta\alpha(\text{av})$ well, which has the three-carbon bridges syn, presumably because of larger nonbonded interactions. The qualitative reason for the energy-optimized structure of **12**⁺⁺ not giving anywhere near the observed $a(\text{N})$ value is clear from the shape of its energy surface, shown in Figure 7c. The optimized structure is nearly planar, but far more pyramidal than that of the optimized structure will be present. Table VI summarizes the energy surfaces calculated in this work and gives results for $\langle \rho(\text{N}) \rangle$ values calculated by Boltzmann averaging, and Table VII compares experimental with calculated $a(\text{N})$ values. It will be noted in Table VI that double nitrogen inversion barriers for **16**⁺⁺ and **7**⁺⁺ are calculated to be very similar, in agreement with experiment. The negative sign of the temperature dependence of $\rho(\text{N})$, corresponding to a decrease in $a(\text{N})$ as the temperature is raised, is consistent with experimental observation for the cations from **16**, **7**, and **19**, and the size is about correct.

Figure 8 shows a plot of averaged $a(\text{N})$ values calculated from $\langle \rho(\text{N}) \rangle$, displayed in the same way as Figure 6. It is qualitatively similar to Figure 6, but averaging has clearly improved the prediction for **12**⁺⁺ and moved the other points around some as well. The calculated $a(\text{N})$ value for **8**⁺⁺[4/u222] is 3.1 G too small,

(17) (a) Pople, J. A.; Beveridge, D. L.; Dobush, P. A. *J. Chem. Phys.* **1967**, *2026*. (b) Pople, J. A.; Beveridge, D. L.; Dobush, P. A. *J. Am. Chem. Soc.* **1968**, *90*, 4201.

(18) Nelsen, S. F. *J. Chem. Soc., Perkin Trans. 2* **1988**, 1005.

(19) Krusic, P. J.; Meaken, P.; Jesson, J. P. *J. Phys. Chem.* **1971**, *75*, 3438.

Table VII. Comparison of Experimental and Calculated $a(N)$ Values (Gauss)

compd[code]	obs	calculated by AMI-UHFQ	
		optimized ^a	averaged ^b
20[hun4]	26.8	26.8	[26.8]
16[221/221]	20.8	20.6	20.2
7[211/222]	20.6	19.7	19.9
17[221/222]	16.1	19.3	18.6 ^c
18[221/322]	14.4	19.2	18.3
19[222/222]	15.1	17.8	17.1
11[222/322]	13.9	16.9	15.7
12[322/322]	13.0	9.7	12.5
21[5/5]	17.6	19.6	20.1
22[5/5m4]	17.1	20.7	20.2
Unsaturated Compounds			
8[4/u222]	21.5	18.8	18.4
6[211/u222]	21.0	21.7	21.2 ^c
13[221/u222]	17.2	21.0	20.5 ^c
14[221/u322]	15.2	20.1	19.1
15[222/u222]	19.2	19.3	18.4
9[322/u222]	16.0	17.7	16.8
10[322/u322]	13.5	14.6	14.0

^a Calculated for the optimized structure only, with $K_N = 477$ G.

^b Calculated by averaging over the energy surface at 25 °C with $K_N = 477$ G unless otherwise noted. ^c Calculated at -78 °C.

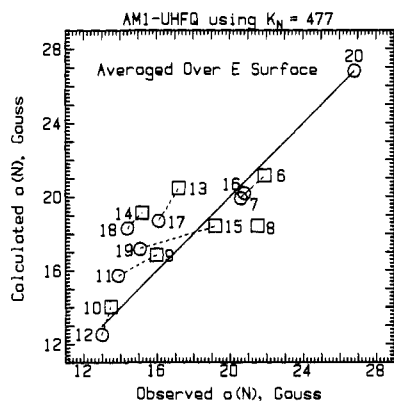


Figure 8. Plot of calculated versus observed $a(N)$ values done as in Figure 6 but by using Boltzmann averaging over one dimensional energy surfaces in $\Delta\alpha(av)$ to obtain $\langle\rho(N)\rangle$.

suggesting that 8^{*+} is calculated to be more planar at N than it actually is. Compound 8^{*+} does differ from the other compounds in having a zero bridge and nitrogens which can flatten (in contrast to 20^{*+}). $a(N)$ values which are too large by 3.9–2.6 G are calculated for the [221/322] systems 18^{*+} and 14^{*+} and [221/222] systems 17^{*+} and 13^{*+} . The other 10 compounds average to a 0.9 G deviation from the line shown, the worst fit being observed for 19^{*+} [222/222] (deviation +2.1 G) and 11^{*+} [222/322] (deviation +1.9 G). Significant contribution of twisted or anti bent conformations, which have lower $\rho(N)$ values at a given $\alpha(av)$ value than the $\theta = 0^\circ$ syn bent ones calculated, to the energy surface would cause the calculated $a(N)$ values to be too large, as observed. Another way of stating the situation is that, to the extent that twisted or anti bent structures contribute, the energy surface drifts away from being “one dimensional” in $\Delta\alpha(av)$, as has been assumed in these calculations. Our general conclusion is that the simple, one dimensional $\Delta\alpha(av)$ energy surface we have assumed is a good description of sesquibicyclic hydrazine cations with smaller ring sizes, but it becomes less good as the sesquibicyclic rings are enlarged. The special constraints of sesquibicyclic hydrazines are necessary for the energy surface to be usefully described as one dimensional in nitrogen pyramidalities.

The calculations give $a(N)$ values which are too high and temperature coefficients which are too low for the bicyclo-[3.3.0]octane derivatives 21^{*+} and 22^{*+} , which can twist more easily than sesquibicyclic compounds. Averaging over syn bent $\theta = 0^\circ$ energy surfaces takes the calculated values farther from

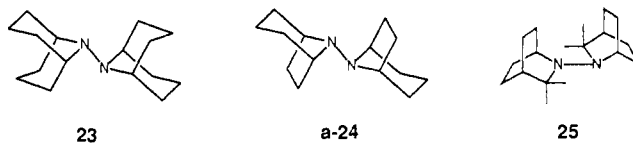
Table VIII. UV Spectral Data of Sesquibicyclic Hydrazine Cation Radicals

compd[code]	Gen ^a	λ_m , nm ^b (ϵ)	$\Delta E(\pi,\pi^*)$, eV	other λ_m (ϵ) values
Saturated Compounds				
16[221/221]	A	321 (700)	3.86	202 (10700)
7[211/222]	B	323 (500)	3.84	
17[221/222]	B	283 (1100)	4.38	204 (8900)
18[221/322]	B	298 (1600)	4.16	
19[222/222]	A ^c	266 (1600)	4.66	204 (9600)
11[222/322]	A	286 (1700)	4.34	208 (10700)
12[322/322]	A	299 (1900)	4.15	208 (10700)
20[Hun4]	C	254 (600)	4.88	
21[5/5]	B ^c	281 (>1100)	4.41	
Unsaturated Compounds				
8[4/u222]	D ^d	302 (400)	4.11	
6[211/u222]	D	266 (600)	4.66	
13[221/u222]	A	280 (1200)	4.43	304 (1000) ^e
14[221/u322]	B	290 (700)	4.28	262 (900), 253 (1100) ^e
15[222/u222]	A ^c	272 (1500)	4.56	286 (1400) ^e
9[322/u222]	A	280 (1200)	4.43	296 (1100) ^e
10[322/u322]	B	292 (1000)	4.25	

^a Method of cation radical generation employed: A, isolated cation radical salt, dissolved in CH_3CN . B, AgNO_3 oxidation in CH_3CN ; ϵ quoted assumes 100% yield of cation radical. C, Electrochemical oxidation in a flow cell (ref 14), taken from the Ph.D. Thesis of Nathan P. Yumibe, University of Wisconsin, Madison, 1985. D, NOPF_6 oxidation in CH_3CN unless otherwise noted; ϵ quoted assumes 100% yield of cation radical. ^b Units for ϵ , $\text{M}^{-1} \text{cm}^{-1}$. ^c From ref 14. ^d Solvent, CH_2Cl_2 . ^e It is not obvious that these are not the π,π^* transitions.

experiment instead of closer. For these bis- N,N' -monocyclic compounds, twisting at the NN bond is unquestionably calculated to be harder than it actually is, as demonstrated by the geometries obtained for the neutral compounds. The energy surfaces for N,N' -dimethyl N,N' -bicyclic or acyclic hydrazines would be much more complex than those for the compounds discussed here because their nitrogens can pyramidalize relatively independently of each other, without increasing the energy much.

Cation Radical UV Spectra. The π,π^* absorption maximum (λ_m ; the transition energy will be called $\Delta E(\pi,\pi^*)$) for tetraalkylhydrazine cation radicals is sensitive to nitrogen pyramidalities.¹⁴ As for $a(N)$, λ_m increases more for syn bending than for anti, for the same orbital-symmetry reasons. Calculations employing the neutral in cation geometry (ncg) method²⁰ for $\text{H}_2\text{NNH}_2^{*+}$ which are forced to assume various amounts of pyramidalization predict regular changes with pyramidalities, and a limited series of compounds seemed to indicate that plots of the experimentally determined quantities $a(N)$ versus λ_m could be useful for determining the amount of pyramidalities at nitrogen. The expected influence of bending at nitrogen on λ_m is demonstrated for anti bent hydrazine cation radicals by the long-wavelength absorption observed for 23^{*+} and 24^{*+} , by the larger λ_m for anti- 24^{*+} than for the less bent syn form, and by the smaller λ_m for 25^{*+} .¹⁴



The series of compounds investigated here greatly extends the number of structurally related syn bent compounds which systematically change $\alpha(av)$, and their UV data are summarized in Table VIII. More than one UV maximum is observed for unsaturated compounds, so alkenyl group framework, π^* absorptions also occur in the region of π,π^* absorption for these compounds. Intense absorption below 210 nm is also observed for several of

the saturated cation radicals. This study demonstrates conclusively that changes in λ_m for sesquibicyclic hydrazine cation radicals is *not* controlled principally by nitrogen pyramidal. Although calculated λ_m for a given compound forced to change its pyramidalities changes regularly, both experiment and calculations give the result that when sesquibicyclic alkyl group ring size is changed, λ_m does not correlate with $\alpha(av)$. The ncg calculations carried out are not reported, because they are basically useless for predicting λ_m of these compounds. AM1 ncg λ_m (and $\Delta E(\pi, \pi^*)$) values do not correlate with experimental ones, in addition to being over 100-nm red-shifted from the observed values. MNDO ncg calculations at AM1 geometries give even larger red-shifts from the experimentally observed numbers. Because MNDO optimizes these cations as being planar at nitrogen, while they are known experimentally to be pyramidal, we have not examined ncg calculations on these geometries.

Conclusions

Changing bicyclic ring sizes in sesquibicyclic hydrazines changes the pyramidalities at N for both n and c forms, and AM1 calculations appear to reproduce the changes usefully well. Free energies for electron loss in acetonitrile correlate well with $\alpha(av)$ calculated by AM1 for the n form; pyramidalities at N and not the details of the sigma orbital structure of the alkyl groups dominates E° . Differences in solvation energies as the alkyl groups are changed vary regularly with the number of carbons in the bicyclic rings. The identity of the alkyl groups and not just $\alpha(av)$ is calculated to be of modest importance in determining the ESR splitting constant $a(N)$. The c forms bend easily enough at N that averaging over the N bending surface is necessary for proper estimation of $a(N)$. The identity of the alkyl groups is substantially more important in determining $\Delta E(\pi, \pi^*)$ for c, and AM1 calculations do not correlate with UV spectral transitions for these compounds. As a result of the great influence of alkyl group structure as well as N pyramidalities on λ_m , correlation of $a(N)$ with λ_m cannot be used to estimate $\alpha(N)$ accurately.

Experimental Section

3,4-Diazatetracyclo[4.2.1.0^{2,5}]non-3-ene (3). Quadricyclane was converted to its diethyl azodicarboxylate adduct by the procedure of Rieber and co-workers,²¹ and the azo compound was prepared in low yield by following the procedure used for preparation of **1**.²²

3,4-Diazatetracyclo[4.2.1.0^{2,5}]non-3-ene Tetrafluoroboric Acid Salt (3H⁺). A solution of 168 mg (1.38 mmol) of **3** in 10 mL of anhydrous ether was treated with 300 μ L of 85% HBF₄·Et₂O (~1.5 equiv based on a density of 1.3 g/mL for the HBF₄·Et₂O solution) under nitrogen, to yield a white precipitate. Ether was removed by cannula and the product was washed twice with fresh ether to give a fine, white powder. Residual ether was removed with a stream of nitrogen, giving 214 mg of 3H⁺BF₄⁻ (1.02 mmol, 74%). ¹H NMR (CD₂Cl₂): δ 5.04 (br s, 1 H), 4.76 (br s, 1 H), 2.79, 2.70 (two overlapping br s, 2 H), 1.7–1.9 (m, 2 H), 1.45 (m, 1 H), 1.0–1.5 (m, 5 H).

2,3-Diazabicyclo[2.1.1]hex-2-ene (4) was received as a gift from D. A. Dougherty.²³

2,3-Diazabicyclo[2.1.1]hex-2-ene tetrafluoroboric acid salt (4H⁺) was prepared from the azo compound as for 3H⁺. ¹H NMR (CD₃CN): δ 5.35 (br s, 2 H), 2.93 (br s, 4 H). ¹H NMR (CD₂Cl₂): δ 5.13–5.5 (two very br overlapping peaks, 2 H), 2.71–3.02 (broadened m, 4 H).

6,7-Diazabicyclo[3.2.2]non-6-ene (5). A mixture of 8.3 g of 1,3-cycloheptadiene (0.089 mol), 9.79 g of diethyl azodicarboxylate (0.089 mol), and 150 mL of anhydrous ether was photolyzed with a Hannovia 450-W mercury lamp at 0–10 °C for 78 h. The adduct obtained was converted to the azo compound by following the procedure for the preparation of **1**,²² increasing the time for the hydrolysis step to 8 h, producing 2.4 g of **5** (0.020 mol, 22% overall yield) as a slightly yellow solid, mp 152 °C after sublimation (lit.²⁴ mp 150).

6,7-Diazabicyclo[3.2.2]non-6-ene tetrafluoroboric acid salt (5H⁺) was prepared from the azo compound as for 3H⁺. ¹H NMR (CD₃CN): δ

5.34 (br s, 2 H), 1.50–2.42 (m, 10 H).

2,7-Diazatetracyclo[5.2.2.1^{3,5}.0^{2,6}]dodec-8-ene (6). A solution of 80.1 mg of **4** (0.98 mmol) in 1 mL of diethyl ether was cooled to 0 °C and 1 equiv of HBF₄·Et₂O (120 μ L) was added via a syringe, causing a white precipitate to form. The ether was removed by cannula, and the residual solvent was removed by rotary evaporation. The remaining material is very sensitive to moisture and should be kept under inert atmosphere at all times. In a glovebag, 1 mL of CD₃CN (to allow monitoring by ¹H NMR) was added, and gas evolution was observed to occur. Adding cyclohexadiene seemed to quench the gas evolution, with formation of some of the Diels–Alder adduct. Protonated adduct was precipitated by adding ether and removing the solvent by cannula. ¹H NMR (CD₃CN): δ 6.50 (m, 2 H), 4.40 (br s, 2 H), 4.30 (br s, 2 H), 2.8–3.0 (m, 1 H), 1.33–2.33 (m, 6 H), 1.22 (d, J /, 1 H). The deprotonated adduct was obtained by adding 5 mL of ether and 2.5 g of crushed NaOH, stirring for 1–2 h at room temperature, filtering, and removing the solvent by rotary evaporation, giving 33.4 mg of crude **6** (0.21 mmol, 21% from **4**). This material was purified by bulb to bulb distillation at room temperature and 0.01 mmHg to a flask at –78 °C to give a white solid. ¹H NMR: δ 6.32–6.39 (m, 2 H), 3.88 (br s, 2 H), 2.86–2.95 (m, 1 H), 2.04–2.11 (m, 2 H), 1.49–1.55 (m, 2 H), 1.20–1.27 (m, 2 H), 0.93 (d, 1 H, J = 7.4 Hz). ¹³C NMR: 134.5 (CH), 65.2 (CH), 52.6 (CH), 43.77 (CH₂, half intensity peak), 29.10 (CH₂, half intensity peak), 25.3 (CH₂). Empirical formula C₁₀H₁₄N₂ was established by high-resolution mass spectroscopy. A higher mass peak was also present in the sample at m/e 207.

2,7-Diazatetracyclo[5.2.2.1^{3,5}.0^{2,6}]dodecane (7). **A. Preparation without Isolating 6.** To 123 mg (1.5 mmol) of **4** dissolved in 0.6 mL of CD₃CN and cooled to 0 °C was added 1 equiv of HBF₄·Et₂O (180 μ L) by syringe. Heating and gas evolution occurred. After the gas evolution slowed (10 min), 1 equiv of 1,3-cyclohexadiene (150 μ L) was added via a syringe. Gas evolution immediately stopped and the solution turned cloudy. This reaction mixture was added to a cool (0 °C) stirring mixture of 1.53 g of KO₂CN=NCO₂K in 10 mL of CH₃CN, followed by 2 mL of HOAc in 3 mL of CH₃CN. The reaction mixture was gradually warmed to room temperature and stirred for 2 days (all operations under N₂). Workup of the reaction (filtration and deprotonation with crushed NaOH in EtOH) showed that there was still some unsaturated adduct present, and the diimide reduction procedure was repeated. The crude product was Kugelrohr distilled at 85 °C, 0.05 mmHg, to give a clear, slightly yellow liquid (30 mg, 12% from **4**). NMR showed traces of the unsaturated adduct still present.

B. Preparation from Isolated 6. A solution of 9.3 mg of **6** (0.0574 mmol) in 10 mL of CH₃CN was cooled to 0 °C under nitrogen and 220 mg (1.13 mmol) of (KO₂CN=N)₂ were added, followed by dropwise addition of 120 mg of HOAc (2 mmol) in 2 mL CH₃CN. After stirring at 0 °C for 1 h, the mixture was gradually warmed to room temperature and then stirred for 12 h. Since all the (KO₂CN=N)₂ did not seem to have reacted, an additional 1 mL of HOAc was added. After stirring for another 16 h, the mixture was filtered through a fine fritted glass filter, and the CH₃CN was removed by rotary evaporation. After stirring with 15 mL of ether and 2 g of crushed NaOH, for 1 h, the mixture was filtered through a fine fritted glass filter to give 5 mg of product as an oil (53% yield from **6**). ¹H NMR (CD₂Cl₂): δ 3.78 (br s, 2 H), 3.00 (br s, 2 H), 1.38–2.35 (m, 12 H). ¹³C NMR (CD₂Cl₂): 63.0 (CH), 49.7 (CH), 44.2 (CH₂, half intensity), 33.0 (CH₂, half intensity), 29.5 (CH₂), 22.2 (CH₂). Empirical formula C₁₀H₁₆N₂ was established by high-resolution mass spectroscopy, but higher m/e peaks were also observed.

2,9-Diazapentacyclo[8.2.2.1^{4,7}.0^{2,9}.0^{3,8}]pentadec-11-ene (8). A mixture of 200 mg of 3H⁺ (0.95 mmol), 10 mL of dry CH₂Cl₂, and 100 μ L of 1,3-cyclohexadiene was stirred for 3 h at ambient temperature, the solvent was removed by rotary evaporation, and the residue was washed with dry ether, producing 0.5 g of crude 8H⁺ (¹H NMR (CD₃CN): δ 6.6–7.07 (very br resonance, width at half-height 30 Hz, 2 H), 3.15–4.45 (broadened resonances, 4 H), 2.02–2.75 (broadened resonance with a width at half-height of 50 Hz, having a protruding sharp peak at 2.4, total 4 H), 1.67–1.88 (m, 2 H), 1.30–1.67 (m, 4 H), 0.74–1.0 (m, 2 H)). This material was stirred with 2.3 g of crushed NaOH in 10 mL of Et₂O for ~1.5 h at room temperature under nitrogen. Filtration through a fine frit and evaporation of the solvent gave 130 mg of **8** (0.64 mmol, 68% from 3H⁺) as a white crystalline solid, mp 133–134 °C. ¹H NMR (CDCl₃): δ 6.6–6.8 (m, 2 H), 3.49 (br s, 2 H), 3.41 (br s, 2 H), 2.64, 2.59 (br d, 1 H), 2.19 (br s, 1 H), 1.63–1.82 (m, 2 H), 1.1–1.43 (m, 5 H), 0.6–0.8 (m, 2 H). ¹³C NMR (CDCl₃): 134.9 (CH), 68.4 (CH), 53.2 (CH), 39.0 (CH), 35.0 (CH₂), 23.7 (CH₂), 21.5 (CH₂). Empirical formula C₁₃H₁₈N₂ was established by high-resolution mass spectroscopy.

2,8-Diazatetracyclo[7.2.2.2^{3,7}.0^{2,8}]pentadec-11-ene (9). One equivalent of HBF₄·Et₂O (24.7 μ L) was added to 18.9 mg of **5** (0.15 mmol) in 0.4 mL of CD₃CN stirring at 0 °C, followed by 1.1 equiv of cyclohexadiene (16 μ L) at room temperature NMR showed complete consumption of **5**

(21) Reiber, N.; Alberts, J.; Lipsky, J. A.; Lemal, D. M. *J. Am. Chem. Soc.* **1969**, *91*, 5668.

(22) Gassman, P. G.; Mansfield, K. T. *Organic Syntheses*; Wiley: New York, 1973; Collect. Vol. 5, p 96.

(23) Chang, M. H.; Jain, R.; Dougherty, D. A. *J. Am. Chem. Soc.* **1984**, *106*, 4211.

(24) Heyman, M. L.; Snyder, J. P. *Tetrahedron Lett.* **1973**, 2859.

after 3 h, and 9H^+ was precipitated with ether. (^1H NMR (CD_3CN): δ 6.68 (m, 2 H), 4.17 (br s, 2 H), 3.50 (br s, 2 H), 1.5-2.2 (m, 12 H), 1.35-1.5 (m, 2 H)). Deprotonation gave 23 mg of **9** (75% from **5**) as a white solid, mp 53-54 °C (after sublimation). ^1H NMR: δ 6.45 (m, 2 H), 3.40 (br s, 2 H), 2.91 (br s, 2 H), 1.48-2.3 (m, 12 H), 1.1-1.28 (m, 2 H). ^{13}C NMR: δ 130.8 (CH), 57.64 (CH), 55.53 (CH), 37.27 (CH₂), 25.43 (CH₂), 22.05 (CH₂), 19.23 (CH₂, half intensity). Empirical formula $\text{C}_{13}\text{H}_{20}\text{N}_2$ was established by high-resolution mass spectroscopy.

2,8-Diazatetracyclo[7.2.2.2^{3,7}.0^{2,8}]pentadecane (11). A mixture of 70 mg of **9** (0.34 mmol), 35 mg of K_2CO_3 , 35 mg of 5% Pd on BaCO_3 , and 8 mL of deaerated reagent-grade ethyl acetate were hydrogenated at atmospheric pressure. The H_2 uptake stopped after 9 mL of H_2 was taken up (~1 equiv). After filtration through Celite, bulb to bulb distillation gave 13 mg (19%) of **11** as a white solid, mp 37 °C. ^1H NMR: δ 2.92 (br s, 2 H), 2.77 (br s, 2 H), 2.0-2.4 (m, 3 H), 1.8-2.0 (m, 4 H), 1.5-1.8 (m, 10 H). ^{13}C NMR (CD_3CN): δ 55.3 (CH, bridgehead C), 54.2 (CH, bridgehead C), 38.5 (CH₂), 30.3 (CH₂), 24.5 (CH₂), 22.0 (CH₂), 20.5 (CH₂, half intensity).

2,8-Diazatetracyclo[7.3.2.2^{3,7}.0^{2,8}]hexadec-12-ene (10). To 0.23 g of **5** (1.83 mmol) in a flask with 10 mL of Et_2O was added 0.28 mL of $\text{HBF}_4 \cdot \text{Et}_2\text{O}$ (~1 equiv) by syringe. The crude 5H^+ was washed with 10 mL of ether, and 3 mL of CH_3CN followed by 0.22 mL of cycloheptadiene were added. After stirring for ~1 week at ambient temperature, the crude 10H^+ was precipitated with ether. (^1H NMR (CD_3CN): δ 6.5 (m, 2 H), 4.07 (br s, 2 H), 3.55 (br s, 2 H), 1.2-2.2 (m, 16 H)). After stirring with 2 g of NaOH in 25 mL of Et_2O for 1 h, filtration, concentration, and recrystallization from Et_2O at -78 °C gave 32 mg of **10** (8% based on **5**) as a white solid, mp 52 °C. ^1H NMR: δ 6.15-6.35 (m, 2 H, olefinic H), 3.42 (br s, 2 H), 3.39 (br s, 2 H),

1.37-2.0 (m, 14 H), 1.06-1.33 (m, 2 H). ^{13}C NMR: δ 129.8 (CH, olefinic C), 59.8 (CH, bridgehead C), 57.0 (CH, bridgehead C), 36.7 (CH₂), 31.1 (CH₂), 20.4 (CH₂), 19.8 (CH₂, half intensity), 19.0 (CH₂, half intensity). Empirical formula $\text{C}_{14}\text{H}_{22}\text{N}_2$ was established by high-resolution mass spectroscopy.

2,8-Diazatetracyclo[7.3.2.2^{3,7}.0^{2,8}]hexadecane (12). A mixture of 150 mg of crude **10**, 33 mg of Pd on BaCO_3 , 42 mg of K_2CO_3 , and 15 mL of deaerated ethyl acetate were hydrogenated until H_2 uptake stopped (total uptake ~6 mL of H_2 in 2 h). After filtration through Celite and removal of solvent by rotary evaporation, 26 mg (17%) of **12** was obtained as a slightly yellow oil which was purified by bulb to bulb distillation. ^1H NMR: δ 2.98 (br s, 4 H), 1.4-2.2 (m, 20 H). ^{13}C NMR: δ 56.4 (CH, bridgehead C), 36.3 (CH₂), 20.6 (CH₂), 20.2 (half intensity). Empirical formula $\text{C}_{14}\text{H}_{24}$ was established by high-resolution mass spectroscopy.

Electrochemical,² ESR,² PES,^{7b} and UV¹⁴ measurements were conducted as previously described. AM1 calculations were carried out on a VAX 8650, using program package AMPAC^{10b} as modified by Timothy Clark.

Acknowledgment. We thank the National Science Foundation for partial financial support of this work under Grant CHE-8415077, the NSF major instrument program, and the National Institutes of Health for support under Grant GM-29549. We thank Prof. D. H. Dougherty (Caltech) for generous supplies of **4**, T. Clark (Erlangen) for versions of AMPAC with UHFQ and AUHF installed, and P. J. Certain and J. M. Standard (Theoretical Chemistry Institute, Wisconsin) for the quantum mechanical treatment of the effects of nitrogen pyramidal on $a(\text{N})$.

Molecular Recognition. 5.¹ Molecular Recognition of Sugars via Hydrogen-Bonding Interaction with a Synthetic Polyhydroxy Macrocycle²

Yasuhiro Aoyama,* Yasutaka Tanaka, and Shuji Sugahara

Contribution from the Department of Chemistry, Nagaoka University of Technology, Kamitomioka, Nagaoka, Niigata 940-21, Japan. Received November 7, 1988

Abstract: The resorcinol-aldehyde cyclotetramer **1a** as a lipophilic polar host solubilizes glycerol and water (neat liquids) and ribose (in an aqueous solution) as polar guests in CCl_4 upon formation of monomeric complexes **1a**-4(glycerol), **1a**-4 H_2O , and **1a**-(ribose) \cdot 2 H_2O , where ribose is bound highly selectively in the α -pyranose form. The extraction of 1,4-cyclohexanediol is also stereoselective, the cis isomer being extracted readily. A pair of hydrogen-bonded OH groups on adjacent benzene rings in **1a** provide the essential binding site for a guest OH group. While glycerol and H_2O are singly bound with such a binding site via hydrogen bonding, α -ribopyranose and cis-1,4-cyclohexanediol are doubly bonded with two binding sites separated by a metaphenylene bridge. Examination of CPK molecular models indicates that such a two-point **1a**-guest interaction is possible when the six-membered ring of a guest has cis OH groups on 1-C and 4-C, as in the case of α -ribopyranose and cis-1,4-cyclohexanediol. The extractabilities, or affinities to **1a**, of various aldopentoses, aldohexoses, and their deoxy derivatives decrease in the following order: fucose (6-deoxygalactose) > 2-deoxyribose > ribose > arabinose \approx rhamnose (6-deoxymannose) >> galactose \approx xylose \approx lyxose \approx mannose \approx glucose. The affinities of sugars are governed by three factors: (1) the stereochemistry of the OH groups on 3-C and 4-C (cis >> trans), (2) the lipophilicity of the substituent on 5-C (CH_3 >> H >> CH_2OH), and (3) the nature of the substituent on 2-C (H > cis-OH > trans-OH, where cis and trans are with respect to the OH group on 3-C). Structural requirements for the formation of stable **1a**-sugar complexes are discussed in terms of maximization of favorable hydrogen-bonding interaction and minimization of unfavorable exposure of the sugar OH groups to bulk solvent.

The hydrogen bonding plays an essential role in biological informational interactions involving proteins, oligo- and polysaccharides, and nucleic acids. Molecular recognition of their

constituents via the host-guest type interaction involving hydrogen bonding is a rapidly growing area. Much attention has been paid to the complexation of amino acids³ and nucleobases and related

(1) Part 4 of this series: Aoyama, Y.; Uzawa, T.; Saita, K.; Tanaka, Y.; Toi, H.; Ogoshi, H.; Okamoto, Y. *Tetrahedron Lett.* **1988**, 29, 5271.

(2) Preliminary accounts of this work: Aoyama, Y.; Tanaka, Y.; Toi, H.; Ogoshi, H. *J. Am. Chem. Soc.* **1988**, 110, 634.

(3) (a) Helgeson, R. C.; Koga, K.; Timko, J. M.; Cram, D. J. *J. Am. Chem. Soc.* **1973**, 95, 3021. (b) Rebek, J., Jr.; Askew, B.; Nemeth, D.; Parris, K. *Ibid.* **1987**, 109, 2432. (c) Aoyama, Y.; Yamagishi, A.; Asagawa, M.; Toi, H.; Ogoshi, H. *Ibid.* **1988**, 110, 4076 and references cited therein.